ORIGINAL ARTICLE

Brain imaging factors associated with progression of subcortical hyperintensities in CADASIL over 2-year follow-up

F. C. Moreton[a], B. Cullen[b], D. A. Dickie[c], R. Lopez Gonzalez[a,d], C. Santosh[e], C. Delles[c] and K. W. Muir[a]

[a]*Institute of Neuroscience and Psychology, Queen Elizabeth University Hospital Glasgow, University of Glasgow, Glasgow;* [b]*Institute of Health and Wellbeing, University of Glasgow, Glasgow;* [c]*Institute of Cardiovascular and Medical Sciences, University of Glasgow, Glasgow;* [d]*Department of Clinical Physics and Bioengineering, Glasgow Royal Infirmary, Glasgow; and* [e]*Institute of Neurological Sciences, Queen Elizabeth University Hospital Glasgow, Glasgow, UK*

Keywords:
CADASIL, stroke, magnetic resonance imaging, cohort study

Received 3 June 2020
revision requested 3 August 2020
Accepted 2 September 2020

European Journal of Neurology 2021, **28:** 220–228

doi:10.1111/ene.14534

Background and purpose: Mutations in the *NOTCH3* gene cause cerebral autosomal dominant arteriopathy with subcortical infarcts and leukoencephalopathy (CADASIL), a cerebral small vessel disease manifesting with stroke, migraine and dementia in adults. The disease displays significant phenotypic variability that is incompletely explained. Early abnormalities in vascular function have been shown in animal models. We postulated that studying changes in vascular function may offer insights into disease progression.

Methods: Twenty-two subjects with CADASIL [50% female, 50 (±11) years] from 19 pedigrees were included in a longitudinal multimodality study using brain magnetic resonance imaging (MRI), clinical measures, neuropsychology and measures of peripheral vascular function. MRI studies included measurement of structural brain changes, cerebral blood flow (CBF) and cerebrovascular reactivity by arterial spin labelling and a CO_2 respiratory challenge.

Results: Over 2 years, new stroke or transient ischaemic attack (TIA) occurred in five (23%) subjects and new significant disability in one (5%). There were significant increases in number of lacunes, subcortical hyperintensity volume and microbleeds, and a decrease in brain volume. CBF declined by 3.2 (±4.5) ml/100 g/min over 2 years. CBF and carotid–femoral pulse wave velocity at baseline predicted change in subcortical hyperintensity volume at follow-up. Carotid intima-media thickness and age predicted brain atrophy. Baseline CBF was lower in subjects who showed a decline in attention and working memory.

Conclusions: Cerebral blood flow predicts radiological progression of hyperintensities and thus is a potential biomarker of disease progression in CADASIL. Over 2 years, there were changes in several relevant imaging biomarkers (CBF, brain volume, lacunes, microbleeds and hyperintensity volume). Future studies in CADASIL should consider assessment of CBF as prognostic factor.

Introduction

Cerebral autosomal dominant arteriopathy with subcortical infarcts and leukoencephalopathy (CADASIL) is due to mutations in the *NOTCH3* gene and is the most common monogenic cause of stroke [1]. Population prevalence has been estimated to be at least 1 in 10 000 [2], but the prevalence of potentially disease-causing *NOTCH3* mutations in public exomes is much higher [3]. There are no effective therapeutic interventions to slow disease progression [4].

The principal manifestations of CADASIL, including stroke, migraine and cognitive dysfunction, are well-described [4]. However, there is marked phenotypic variability, even in individuals with the same mutation. This hampers individual prognostication

Correspondence: F. C Moreton, Institute of Neuroscience and Psychology, University of Glasgow, Imaging Centre of Excellence, Queen Elizabeth University Hospital, Glasgow, G51 4LB, UK (tel.: ++447709336232; e-mail: fiona.moreton@glasgow.ac.uk).

© 2020 The Authors. *European Journal of Neurology* published by John Wiley & Sons Ltd on behalf of European Academy of Neurology
This is an open access article under the terms of the Creative Commons Attribution-NonCommercial-NoDerivs License, which permits use and distribution in any medium, provided the original work is properly cited, the use is non-commercial and no modifications or adaptations are made.

and impedes clinical trials since clinical end-point variability and slow progression greatly inflate sample size in any potential therapeutic trial [5].

There is a limited understanding of the factors that underlie clinical progression. The clinical predictors include age and dementia, but only current smoking and hypertension may be modifiable [6,7]. Magnetic resonance imaging (MRI) markers of cerebral small vessel disease such as lacunes [8] and atrophy [9] have been shown to predict clinical worsening to varying degrees [10]. However, these may manifest fairly late in the disease pathway.

Impaired clearance of the mutated NOTCH3 extracellular domain appears to lead to toxic protein aggregation, cellular damage and degeneration of small cerebral vessels and pericytes [11,12]. This is associated with vascular dysfunction [13,14] that precedes histological evidence of brain damage in mouse models [12] In a cross-sectional study in subjects with CADASIL, we showed that impaired cerebral and peripheral vasoreactivity were associated with higher numbers of lacunes [15]. If changes in vascular function occur early, are pathophysiologically relevant and are amenable to interventions, this may make them excellent biomarkers [12].

Therefore, we aimed to investigate longitudinal changes in vascular function in people with CADASIL. We aimed to establish if they are relevant in clinical or radiological progression of CADASIL, and whether they have merit for inclusion in future studies.

Materials and methods

Study cohort

Subjects were prospectively recruited between May 2013 and November 2013 from a specialist neurovascular genetics clinic at the Queen Elizabeth University Hospital Glasgow, United Kingdom. Eligible subjects were aged 18 years or over with a genetic diagnosis of CADASIL. Exclusion criteria included contraindications to MRI, current use of calcium channel blockers or angiotensin-converting enzyme inhibitors, and type II respiratory failure. Subjects provided written informed consent.

The study was approved by the West of Scotland Research Ethics Service (12/WS/0295). The study was conducted in accordance with standards laid down in the Helsinki Declaration of 1975 (revised 1983). Subjects underwent study procedures at recruitment, 1 and 2 years, as well as telephone calls at 6 monthly intervals to ensure no clinical changes were missed.

Clinical and demographic data, including cardiovascular risk factors, were collected during the study period. A history of transient ischaemic attacks (TIA) or stroke, psychiatric disorders, depression, migraine, seizures or other medical conditions was obtained at each review. Neurological impairment was assessed using the National Institutes of Health Stroke Scale [16]. Global disability was assessed by the modified Rankin Scale (mRS), using the structured Rankin Focused Assessment tool [17]. Moderate or severe disability was defined as mRS $\geq$ 3.

Study procedures

All peripheral vascular tests took place within a temperature-controlled room (22–24°C) using a standardised protocol. Vascular phenotyping included ultrasound assessment of flow-mediated dilatation (FMD) of the brachial artery and ultrasound measurement of carotid intima-media thickness (CIMT). Carotid-femoral pulse wave velocity (PWV) was measured using applanation tonometry (SphygmoCor; AtCor Medical, Sydney, Australia). Detailed description of methods and analysis used in this study have been published previously [15] and are included in Appendix S1.

Neuropsychological assessment was carried out over one or two sessions at each time-point by a specialist clinical neuropsychologist (B.C.), and included standardised tests of estimated premorbid ability, global cognitive function, processing speed, verbal and visual attention and working memory, verbal and visual episodic memory, visuospatial function, verbal fluency, verbal reasoning and executive function. The domains of speed, attention/working memory and executive function were chosen *a priori* for analysis. Composite domain scores were derived from individual tests by converting raw scores to standardised scores (corrected for age, or age and education, with reference to published normative tables). The mean of scores within a particular cognitive domain was then calculated; higher composite scores represented better performance. Details of the components of each composite score can be found in Appendix S1. Trail-making B minus A time was also analysed separately (measured in seconds, with higher values indicating worse performance). For analysis, change in composite scores between year 2 and baseline were categorised into decline or improvement for comparison with vascular markers.

Brain MRI acquisition

Subjects were scanned on a 3T MRI GE Signa Excite HD scanner with an eight- channel head coil (GE Medical Systems, Milwaukee, WI, USA). MRI sequences used for this study have been reported in detail

© 2020 The Authors. *European Journal of Neurology* published by John Wiley & Sons Ltd on behalf of European Academy of Neurology

previously [15] and are included in Appendix S1. Briefly, the protocol included high-resolution millimetric, three-dimensional (3D), T1-weighted, 5 mm T2-weighted fluid-attenuated inversion recovery (FLAIR), T2*-weighted susceptibility-weighted angiography (SWAN) and 3D magnetic resonance angiography. 3D pseudo-continuous arterial spin labelling MRI was performed with the patient breathing 15 l/min air, and repeated whilst breathing 40 l/min of 6% CO_2/air. A close-fitting gas mask (Ref 1141; Intersurgical, Wokingham, United Kingdom) and unidirectional breathing circuit (Ref 2013014; Intersurgical) were used to administer the gases. Expiratory ports were closed, and gauze swabs and tape were used to improve fit. Gas concentrations and patient observations were recorded throughout (Veris Vital Signs Monitor; MEDRAD, Indianola, IA, USA).

Image processing

Cerebral microbleeds, lacunes and subcortical hyperintensities (SHs) were defined as per recent neuroimaging standards [18]. Location and number of microbleeds were recorded using the Microbleed Anatomical Rating Scale at baseline [19] using SWAN images and with reference to other sequences. Incident microbleeds identified on serial scans were added to the baseline total by one rater.

FMRIB software library (FSL) version 5.0 tools, including SIENAX and SIENA, were used to determine intracranial cavity volume (ICCV) from SWAN images and brain volume from T1-weighted images [20–22]. Changes in global brain volume between baseline and year 2 [percentage brain volume change, (PBVC)] were calculated for all subjects using SIENA.

Hyperintense signal abnormalities on FLAIR in white matter, grey matter and brainstem were termed SHs [18]. SHs were analysed on FLAIR images. SH volumes were initially estimated as described previously [23]. These initial estimates were then edited by a trained rater. The optimal FLAIR threshold for each patient was chosen by inspection of the baseline map, and used for the following years. The total volume of SH was normalised for ICCV in each patient [normalised SH volume = (SH volume/ICCV) × 100].

Baseline lacunes were counted and segmented manually using two-dimensional and 3D thresholding tools on 3D T1-weighted images (Analyze version 11.0; AnalyzeDirect, Stilwell, KS, USA).

Incident lacunes were identified using difference imaging from T1-weighted images obtained at baseline and follow-up. SWAN maps were registered to T1-weighted, skull stripped and used to mask the T1-weighted image (using FSL tools) [21]. The baseline brain image was registered to Montreal Neurological Institute 1-mm brain template with 6 degrees of freedom. Year 1 and 2 brain images were then registered to this image with 12 degrees of freedom. The images were bias corrected, and follow-up images were subtracted from baseline image to create a difference map at year 1 and year 2. The difference map was reviewed, with reference to original images, to identify new lacunes (Fig. 1).

At each time-point, structural scans, SH masks and arterial spin labelling (ASL) scans were coregistered (Analyze version 11). The transformed T1-weighted image was segmented into parenchyma (brain), grey, and white matter masks [24]. SH pixels were removed from grey and white matter masks. Quantitative cerebral blood flow (CBF) maps were generated using an

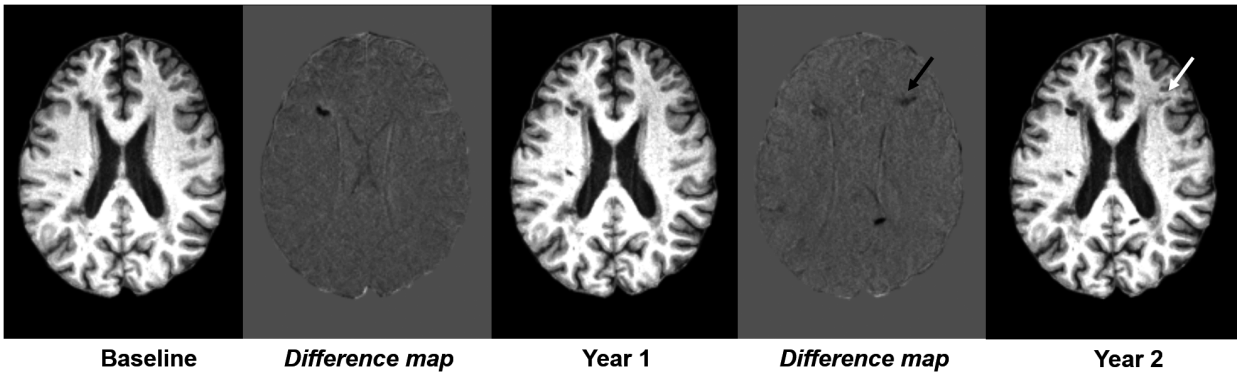

Figure 1 Identification of new lacunes. T1-weighted images at each time-point were coregistered to the Montreal Neurological Institute template and bias corrected. This allowed creation of difference maps to identify new areas of signal change. In each new area, reference was made to original T1-weighted images, and to other available sequences to confirm if it was a new lacune. The arrow highlights an area of signal change, which represented new white matter hyperintensity and a perivascular space. One new lacune can be seen on each difference map as a black area.

© 2020 The Authors. *European Journal of Neurology* published by John Wiley & Sons Ltd on behalf of European Academy of Neurology

in-house macro for Image J (Rasband, W.S., ImageJ, National Institutes of Health, Bethesda, MD, USA; http://imagej.nih.gov/ij/, 1997–2014.) Masks were then applied to CBF maps to measure CBF and cerebrovascular reactivity (CVR) in brain regions. Change in CBF (%ΔCBF) was corrected for change in end-tidal CO_2 ($EtCO_2$) to calculate cerebrovascular reactivity (CVR_{ASL}):

$$CVR_{ASL} = \frac{CBF_{hypercapnia} - CBF_{normocapnia}}{CBF_{normocapnia}} \times \frac{100}{EtCO_{2hypercapnia} - EtCO_{2\ normocapnia}}$$

Expiratory gas data were used if $EtCO_2$ whilst breathing air was between 3.5 and 6.5%, suggesting reasonable mask seal.

Statistical analysis

Statistical analysis was performed with IBM SPSS version 24 (IBM, Armonk, NY, USA).

A composite clinical outcome (based on other CADASIL studies [25]) at 2 years was used: a new stroke or TIA or new moderate-to-severe disability (mRS 3–5) in those without significant disability (mRS 0–2) at baseline, or worsening of mRS of 1 or more grades in those with significant disability (mRS 3–5) at baseline.

Data were both inspected for normality and assessed with Shapiro-Wilks test. Box plots were examined for outliers. Change in continuous variables over time was analysed with a one-way repeated measures ANOVA. Where there was a significant change, a *post hoc* contrast between baseline and year 2 was performed. Related-samples Friedman two-way tests were used for non-parametric data. When there was a significant change, pairwise comparisons with a Bonferroni correction for multiple comparisons was used. PBVC between baseline and year 2 was assessed with a one-way *t* test.

Associations of outcome variables with baseline variables was determined using Spearman rank correlations. For categorical outcome variables, association with baseline variables was determined with independent *t* tests for normal data or Mann-Whitney *U* tests for non-normal data.

Results

Cohort demographics

Twenty-two subjects were recruited [50% female, mean age 50 (standard deviation ± 11) years] from 19 pedigrees. Twenty subjects had 'classical' mutations in epidermal growth factor-like repeats (EGFr) 1 to 6, and two in EGFr 7 to 34 [3]. Cohort characteristics are shown in Table 1. Two subjects declined MRI at year 2. One patient developed acute leukaemia and did not complete all investigations at year 2 but did undergo MRI.

Clinical changes

During the study, a new stroke or TIA occurred in five subjects (23%). New moderate or severe disability occurred in one subject (5%). The composite clinical outcome occurred in five subjects (23%) by study completion.

There were no significant changes over time in executive function, attention and working memory or Trails B minus A time (see Appendix S2, Table S1). Processing speed differed significantly over time (Table 1). *Post hoc* pairwise comparisons showed differences were due to an improvement in scores at year 1 compared to baseline ($P = 0.003$) and a decline between year 1 and 2 ($P = 0.011$). There was no overall difference between baseline and year 2 ($P = 1$).

Structural MRI changes

Normalised SH volume increased over the study (Table 1). There was a mean increase of 0.57% [95% confidence interval (CI): 0.39 to 0.75, $P < 0.001$] between baseline and year 2. There was a significant decline in brain volume from baseline and year 2, measured using SIENA, with a PBVC of −0.87% (95% CI: −0.4 to −1.3, $P = 0.001$). Numbers of lacunes and microbleeds significantly increased over the study period. Three subjects had no lacunes at baseline, and none of these subjects developed incident lacunes during the study period, although one subject (aged 30 years) did not have imaging at year 2. (See Appendix S2, Figure S1, for spaghetti plots of MRI variables).

Vascular changes

Grey matter CBF changed over the study period (Table 1). There was a mean decrease from baseline (49 ± 10 ml/100 g/min) to year 2 (45 ± 9 ml/100 g/min) of 3.2 ml/100 g/min (95% CI: 0.6 to 5.7, $P = 0.019$). Brain CVR, FMD, PWV and blood pressure did not significantly change over the study (Table 1). CIMT significantly increased over the study period, with a mean increase of 0.06 mm (95% CI: 0.02 to 0.10, $P = 0.01$) between baseline and year 2 (see Appendix S2, Figure S2 for spaghetti plots of key vascular and neuropsychological variables).

© 2020 The Authors. *European Journal of Neurology* published by John Wiley & Sons Ltd on behalf of European Academy of Neurology

Table 1 Change over study period in MRI, neuropsychological and vascular measures with repeated measures comparisons

	n[a]	Baseline	Year 1	Year 2	P value[b]
Clinical characteristics					
Age, years, median [range]	22	53 [26–67]	—	—	—
Female, n (%)	22	11 (50%)	—	—	—
Active smoking, n (%)	22	7 (32%)	—	—	—
Years of education, median [IQR]	22	12 [11–15]	—	—	—
History of TIA or stroke, n (%)	22	11 (50%)	11 (50%)	12 (55%)	—
mRS ≥ 3, n (%)	22	3 (14%)	3 (14%)	4 (18%)	—
Neuropsychological measures					
ToPF estimated IQ, mean (SD)	22	97 (13)	—	—	—
Processing speed, median [IQR], composite z-score	18	−0.2 [−1.6 to 0.5]	0.4 [−1.0 to 0.7]	−0.1[−0.9 to 0.5]	**0.001**
Structural MRI measures					
No. of lacunes, median [IQR]	19	5 [2 to 15]	5 [3 to 18]	6 [3 to 24]	**<0.001**
No. of microbleeds, median [IQR]	20	1 [0 to 5]	2 [0 to 7]	3 [0 to 9]	**<0.001**
Normalised subcortical hyperintensity volume, %, mean (SD)	19	8.2 (3.1)	8.5 (3.0)	8.8 (3.1)	**<0.001**
Normalised brain volume, L, mean (SD)	19	1.54 (0.09)	1.53 (0.08)	1.53 (0.06)	—
Vascular measures					
Grey matter CBF, ml/100 g/min, mean (SD)	15	48 (10)	44 (7)	45 (9)	**0.022**
Brain CVR, %/CO_2, mean (SD)	10	10.5 (9.6)	11.8 (10)	7.5 (6.5)	0.321
CIMT, mm, mean (SD)	18	0.63 (0.1)	0.64 (0.1)	0.68 (0.1)	**0.009**
FMD, %, mean (SD)	12	4.1 (1.4)	4.4 (2.1)	4.7 (1.6)	0.564
PWV, m/S, mean (SD)	14	7.9 (1.1)	7.7 (1.0)	8.1 (1.0)	0.116
Systolic BP, mmHg, mean (SD)	22	120 (11)	125 (12)	121 (15)	0.128

P values <0.05 are shown in bold typeface. BP, blood pressure; CBF, cerebral blood flow; CIMT, carotid intima-media thickness; CVR, cerebrovascular reactivity; FMD, flow-mediated dilatation; IQ, intelligence quotient; IQR, interquartile range; MRI, magnetic resonance imaging; mRS, modified Rankin Scale; PWV, pulse wave velocity; SD, standard deviation; TIA, transient ischaemic attack; ToPF, test of premorbid functioning. [a]Number where data are available at all three time-points. [b]Normally distributed data expressed as mean (SD) and comparisons made with repeated measures ANOVA. Non-parametric data are expressed as median [IQR] and comparisons were made with the Friedman test.

Relationship of vascular measures with clinical and neuropsychological changes

There was no statistically significant difference in baseline CBF, CVR, FMD, CIMT or PWV in subjects who did obtain the composite clinical outcome compared to those who did not (Appendix S2, Table S2). No factor significantly correlated with change in processing speed, executive function, or Trails B minus A time. Baseline grey matter CBF was lower in subjects who showed a decline in attention and working memory [decline, 40 (±8) ml/100 g/min vs. no decline 52 (±6) ml/100 g/min, $P = 0.009$; see Appendix S2, Table S3].

Relationship of vascular measures with structural MRI changes

Lower CBF at baseline was correlated with increased normalised SH volume change at year 2 (Table 2 and Fig. 2a). At baseline, grey matter CBF and normalised SH volume were not significantly correlated ($n = 17$, $r_s = -0.417$, $P = 0.096$), but they were at both 1-year ($n = 22$, $r_s = -0.483$, $P = 0.023$) and 2-year follow-up ($n = 19$, $r_s = -0.591$, $P = 0.008$).

Lower PWV at baseline was also correlated with higher normalised SH volume change by year 2 (Table 2), but PWV did not correlate with normalised SH volume at individual time-points (data not shown). Higher age and CIMT at baseline were correlated with an increased rate of brain atrophy (Table 2).

No baseline vascular marker (FMD, CBF, CVR, CIMT, PWV) significantly predicted number of incident lacunes or incident microbleeds (Appendix S2, Table S4).

Discussion

In this longitudinal study in a cohort of subjects with CADASIL, baseline CBF was predictive of change in subcortical hyperintensity volume over a 2-year follow-up period. CBF merits further assessment as both a potential biomarker of disease progression and a therapeutic target.

Our study demonstrated a longitudinal decline in CBF in CADASIL patients. A 6% decline in CBF over 2 years is higher than that reported in healthy populations of 0.45% per annum, also using ASL [26]. ASL offers an evolving, non-invasive and repeatable method of perfusion imaging. This high percentage change over a short time period suggests this marker may have utility in short clinical trials,

© 2020 The Authors. *European Journal of Neurology* published by John Wiley & Sons Ltd on behalf of European Academy of Neurology

Table 2 Baseline vascular markers predicting change in structural magnetic resonance imaging from baseline to year 2

		Change in normalised SH volume (%)	Percentage brain volume change (%)
Age, years	Correlation coefficient	−0.134	−0.700*
	Significance (2-tailed)	0.585	0.001
	n	19	19
Grey matter CBF, ml/100 g/min	Correlation coefficient	−0.557*	0.354
	Significance (2-tailed)	0.031	0.196
	n	15	15
White matter CBF, ml/100 g/min	Correlation coefficient	−0.643*	0.236
	Significance (2-tailed)	0.01	0.398
	n	15	15
CIMT, mm	Correlation coefficient	0.215	−0.525*
	Significance (2-tailed)	0.378	0.021
	n	19	19
PWV, m/s	Correlation coefficient	−0.481*	−0.461
	Significance (2-tailed)	0.043	0.054
	n	18	18

CBF, cerebral blood flow; CIMT, carotid intima-media thickness; PWV, pulse wave velocity; SH, subcortical hyperintensities. *P value < 0.05.

although the small study limits the precision of the estimates in this study.

We found subjects with lower CBF at baseline had a greater increase in normalised SH volume over time, suggesting a causal relationship. However, given subcortical hyperintensities are often a very early finding in CADASIL, preceding both other radiological changes and often symptoms [27], this relationship is unlikely to be a simple linear one.

Subjects with lower CBF at baseline had a decline in attention and working memory over the study. This was not seen on other measures of subcortical cognitive function, such as processing speed, which may reflect the limited changes in these measures over this time period. Lower CBF and brain CVR was also seen in those who obtained the composite clinical outcome (i.e. suffered incident strokes or dementia), but this was not significant (see Appendices S1 and S2, Table 2), and the small group numbers hamper interpretation.

Altered CBF in CADASIL is a mechanistically plausible biomarker, but previous studies of brain perfusion have been limited, mainly by the requirement for radiation or contrast. NOTCH3 extracellular domain acts as a nidus for deposition of other proteins, and accumulates in pericytes and vascular smooth muscles cells, leading to vessel damage and dysfunction [11]. The endothelial dysfunction may relate to disruption of pericytes in capillaries [28], resulting in impaired control of CBF [29]. It is postulated that capillary dysfunction leads to a decrease in oxygen extraction efficiency, which can initially be compensated for by increasing CBF and potentially by reducing capillary transit time heterogeneity [30]. Early positron emission tomography studies demonstrated preserved and even hyperaemic cortical perfusion in patients under the age of 30 years, and it was suggested that age 30 years was the transition zone for the decline in CBF [31].

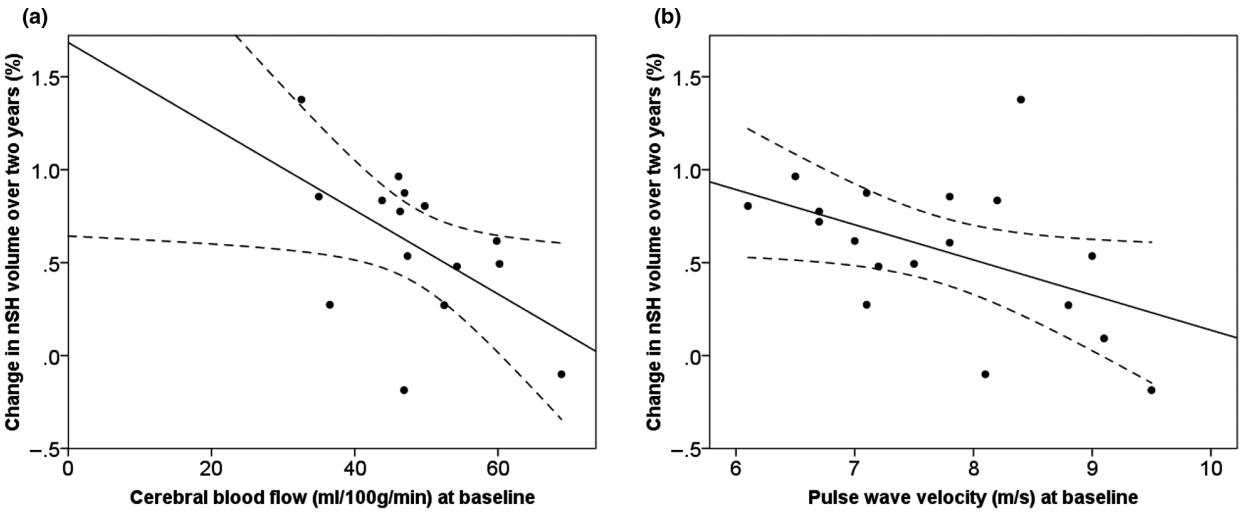

Figure 2 Predictors of change in normalised subcortical hyperintensity (nSH) volume. (a) Lower cerebral blood flow at baseline was associated with a higher increase in nSH volume at 2 years. (b) Lower pulse wave velocity at baseline demonstrated a similar relationship. Line of best fit (solid line) and 95% confidence intervals of the mean (dashed lines) are shown.

© 2020 The Authors. *European Journal of Neurology* published by John Wiley & Sons Ltd on behalf of European Academy of Neurology

As damage to vessels accumulates, CBF may decrease to minimise functional shunting and maintain flow-metabolism coupling. Attenuated functional hyperaemia is seen in 6-month CADASIL mouse models even before arteriolar damage is incurred [12], suggesting unmasking of capillary dysfunction by additional demands. Later in the disease, there is likely a critical point at which the extent of damage leads to a drop in CBF and acceleration of the disease process. SPECT studies have shown global hypoperfusion that appeared worse in older and more severely affected subjects [32], but perfusion results were not always clearly related to clinical outcomes [33].

The evidence for the relationship between CBF and hyperintensities remains conflicting. A recent cross-sectional study using ASL suggested CBF in white matter hyperintensities was correlated with global cognitive function, and was a better predictor than mean diffusivity [34]. An immunotherapy study in CADASIL mice, showed that binding of a mouse monoclonal antibody to the NOTCH3 extracellular domain protected against impaired CBF flow responses to both neural activity and vasodilators, although this did not influence deposition of granular osmiophilic material or stop white matter lesion development [35]. High-field MRI combining both ASL and direct visualisation of small vessels in studies including earlier, pre-symptomatic subjects may allow investigation of this relationship in more detail. Further validation against clinical events over time in a larger sample would be required to strengthen the case for CBF to be considered a potential surrogate end-point.

Cerebral blood flow and vascular haemodynamics may also be a target for therapeutics in CADASIL. Currently, treatment is limited to conventional stroke preventative treatments and addressing risk factors. Whilst drugs that temporarily increase or improve vascular haemodynamics may hypothetically offer some symptomatic benefit, for example acetazolamide [36], disease modifying therapeutics are likely to need to target the drivers of impaired vascular function. The immunotherapy study in CADASIL mice had beneficial effects on cerebrovascular function. Our recent study using biopsy samples from subjects with CADASIL as well as CADASIL mice models, showed aberrant responses in the Notch3-Nox5/ER stress/ROCK signalling pathway leading to impaired vasorelaxation, blunted vasoconstriction and hypertrophic remodelling [14]. Administration of inhibitors of Notch3 function including fasudil resulted in amelioration of impaired vasorelaxation. Therefore, preclinical studies are already focusing on this for therapeutic targets, and our ability to measure these changes in human subjects is important.

Changes in structural MRI markers were not the direct focus of this study but were similar to those reported in a recent longitudinal cohort study of 160 subjects with CADASIL [37]. In that study, the mean annualised rate of white matter hyperintensities volume increase over 3 years was 0.28% of the intracranial cavity, and the annualised rate of brain volume loss was 0.45%, and these variations were statistically significant from around 18 months. In our study of 22 subjects, the mean annualised change was 0.29% (for subcortical hyperintensities) and 0.44%, respectively. Our replication in a smaller cohort supports the generalisability of these measures when performed using automated or semiautomated techniques and supports their use in multicentre clinical trials. Limited change in clinical and neuropsychological markers concurs with larger datasets [10,37] and confirms the challenge of their use over short follow-up periods. Practice effects on cognitive measures are relevant and likely explain the improvement in processing speed between baseline and year 1, and in a small cohort, patient mood and fatigue may introduce additional variability.

Markers of large-vessel health were also explored in this study. There was a suggestion that low PWV at baseline was associated with increase of SH volume over time. This would be a surprising relationship, and may reflect the limited range of values for PWV in this study. High aortic stiffness, represented by higher PWV measurements, is generally thought to have an adverse effect on the brain being associated with lower CBF in non-CADASIL populations [38]. However, these populations are generally older, with higher rates of hypertension and a wider range of PWV readings. CIMT results were consistent with previous observations in both general and CADASIL populations [39,40]. CIMT at baseline (and increasing age) was associated with brain atrophy in this study. CIMT increased during the study period. Increase in CIMT over time may be seen with aging; however, measurement error for CIMT can be in the region of 0.03 to 0.05 mm [40], and thus, correlation with individual changes in imaging or clinical parameters should be interpreted cautiously. Given the known interactions of CADASIL with factors such as smoking and hypertension [7], our findings may support that large vessel vascular function interactions warrant ongoing study.

The methodological strengths of this study include the prospective design and the quantitative assessment of normalised SH volume and brain atrophy, which demonstrated high concurrence with other studies. All MRI scans were performed on the same scanner, and all neuropsychological tests by the same assessor.

The major limitation of this study is the small number of subjects. This reflects the ongoing apparent

© 2020 The Authors. *European Journal of Neurology* published by John Wiley & Sons Ltd on behalf of European Academy of Neurology

clinical rarity of CADASIL, despite evidence of significant underdiagnosis. All subjects underwent extremely detailed assessment. Small numbers mean we have to be cautious in drawing definitive conclusions, but the aim of this study was to explore potential measures that may warrant further research. There were insufficient subjects to explore the effect of typical and atypical mutations, which may have phenotypic relevance [3]. Issues with reliability of gas delivery methods and monitoring need to be considered going forward, as not all subjects could have accurate CO_2 levels measured [41]. A ceiling effect for normalised SH volume was not accounted for in this study but may be relevant in other cohorts. Not all associations found in our baseline study could be explored further at year 2 follow-up.

In conclusion, we found CBF to predict progression of subcortical hyperintensity volume over a 2-year period, observed longitudinal changes in CBF many times larger than changes seen in non-CADASIL subjects and, in addition, confirmed progression of several structural indices in CADASIL over a 2-year period. CBF may offer a therapeutic target and biomarker of relevance and should be explored in larger trials.

Acknowledgements

The authors offer their thanks to all the subjects and their families for their dedication and patience. They thank Dr. John Mclean, Superintendent Isobel MacDonald, and the neuroradiographers and stroke research nurses for their assistance. They also thank Professor Christian Schwarzbauer for his help designing the respiratory challenge experiments and Dr. Krishna Dani for support with MRI analysis. The study was funded by a project grant from the Chief Scientist Office, Scotland (ETM/244). C.D. and K.W.M. were also supported by a BHF Centre of Excellence award (RE/18/6/32417). D.A.D. is funded by a Stroke Association postdoctoral fellowship (TSA/PDF/2017/01).

Disclosure of conflicts of interest

K.W.M. reports personal fees and non-financial support from Boehringer Ingelheim, personal fees from Bayer, Daiichi Sankyo, and ReNeuron, outside the submitted work. D.A.D. reports grants from the Stroke Association and personal fees from MicroTransponder Inc., outside the submitted work.

Data availability statement

The data that support the findings of this study are available on request from K.W.M. The data are not publicly available due to privacy or ethical restrictions.

Supporting Information

Additional Supporting Information may be found in the online version of this article:

Appendix S1. Methods

Table S1. Change over study period in neuropsychological measures with repeated measures comparison

Table S2. Baseline vascular and radiological markers in those obtaining the clinical composite outcome

Table S3. Baseline vascular and radiological markers in subjects in those with decline in attention/working memory

Table S4. Baseline vascular markers predicting change in structural MRI from baseline to year 2 – lacunes and microbleeds

Figure S1. Spaghetti plots of change in MRI variables over 2 years

Figure S2. Spaghetti plots of change in key vascular and neuropsychological variables over 2 years

References

1. Joutel A, Corpechot C, Ducros A, *et al*. Notch3 mutations in CADASIL, a hereditary adult-onset condition causing stroke and dementia. *Nature* 1996; **383:** 707–710.
2. Moreton FC, Razvi SSM, Davidson R, Muir KW. Changing clinical patterns and increasing prevalence in CADASIL. *Acta Neurol Scand* 2014; **130:** 197–203.
3. Rutten JW, Dauwerse HG, Gravesteijn G, *et al*. Archetypal NOTCH3 mutations frequent in public exome: implications for CADASIL. *Ann Clin Transl Neurol* 2016; **3:** 844–853.
4. Chabriat H, Joutel A, Dichgans M, Tournier-Lasserve E, Bousser MG. Cadasil. *Lancet Neurol* 2009; **8:** 643–653.
5. Peters N, Herzog J, Opherk C, Dichgans M. A two-year clinical follow-up study in 80 CADASIL subjects. *Stroke* 2004; **35:** 1603–1608.
6. Chabriat H, Herve D, Duering M, *et al*. Predictors of clinical worsening in cerebral autosomal dominant arteriopathy with subcortical infarcts and leukoencephalopathy: prospective cohort study. *Stroke* 2016; **47:** 4–11.
7. Adib-Samii P, Brice G, Martin RJ, Markus HS. Clinical spectrum of CADASIL and the effect of cardiovascular risk factors on phenotype: study in 200 consecutively recruited individuals. *Stroke* 2010; **41:** 630–634.
8. Liem MK, van der Grond J, Haan J, *et al*. Lacunar infarcts are the main correlate with cognitive dysfunction in CADASIL. *Stroke* 2007; **38:** 923–928.
9. Jouvent E, Viswanathan A, Mangin J-F, *et al*. Brain atrophy is related to lacunar lesions and tissue microstructural changes in CADASIL. *Stroke* 2007; **38:** 1786–1790.

© 2020 The Authors. *European Journal of Neurology* published by John Wiley & Sons Ltd on behalf of European Academy of Neurology

10. Benjamin P, Zeestraten E, Lambert C, *et al*. Progression of MRI markers in cerebral small vessel disease: sample size considerations for clinical trials. *J Cereb Blood Flow Metab* 2016; **36:** 228–240.
11. Joutel A. The NOTCH3ECD cascade hypothesis of cerebral autosomal-dominant arteriopathy with subcortical infarcts and leukoencephalopathy disease. *Neurol Clin Neurosci* 2015; **3:** 1–6.
12. Joutel A, Monet-Lepretre M, Gosele C, *et al*. Cerebrovascular dysfunction and microcirculation rarefaction precede white matter lesions in a mouse genetic model of cerebral ischemic small vessel disease. *J Clin Investig* 2010; **120:** 433–445.
13. Dziewulska D, Lewandowska E. Pericytes as a new target for pathological processes in CADASIL. *Neuropathology* 2012; **32:** 515–521.
14. Neves KB, Harvey AP, Moreton F, *et al*. ER stress and Rho kinase activation underlie the vasculopathy of CADASIL. *JCI Insight* 2019; **4:** e131344.
15. Moreton FC, Cullen B, Delles C, *et al*. Vasoreactivity in CADASIL: comparison to structural MRI and neuropsychology. *J Cereb Blood Flow Metab* 2018; **38:** 1085–1095.
16. Brott T, Adams HP, Olinger CP, *et al*. Measurements of acute cerebral infarction: a clinical examination scale. *Stroke* 1989; **20:** 864–870.
17. Saver JL, Filip B, Hamilton S, *et al*. Improving the reliability of stroke disability grading in clinical trials and clinical practice. *Stroke* 2010; **41:** 992–995.
18. Wardlaw JM, Smith EE, Biessels GJ, *et al*. Neuroimaging standards for research into small vessel disease and its contribution to ageing and neurodegeneration. *Lancet Neurol* 2013; **12:** 822–838.
19. Gregoire SM, Chaudhary UJ, Brown MM, *et al*. The Microbleed Anatomical Rating Scale (MARS): reliability of a tool to map brain microbleeds. *Neurology* 2009; **73:** 1759–1766.
20. Jenkinson M, Smith S. A global optimisation method for robust affine registration of brain images. *Med Image Anal* 2001; **5:** 143–156.
21. Smith SM, Jenkinson M, Woolrich MW, *et al*. Advances in functional and structural MR image analysis and implementation as FSL. *NeuroImage* 2004; **23** (S1)**:** 208–219.
22. Smith SM, Zhang M, Jenkinson M, *et al*. Accurate, robust and automated longitudinal and cross-sectional brain change analysis. *NeuroImage* 2002; **17:** 479–489.
23. Dawson J, Broomfield N, Dani K, *et al*. Xanthine oxidase inhibition for the improvement of long-term outcomes following ischaemic stroke and transient ischaemic attack (XILO-FIST) – protocol for a randomised double blind placebo-controlled clinical trial. *Eur Stroke J* 2018; **3:** 281–290.
24. Zhang Y, Brady M, Smith S. Segmentation of brain MR images through a hidden Markov random field model and the expectation-maximization algorithm. *IEEE Trans Med Imaging* 2001; **20:** 45–57.
25. Chabriat H, Hervé D, Duering M, *et al*. Predictors of clinical worsening in cerebral autosomal dominant arteriopathy with subcortical infarcts and leukoencephalopathy: prospective cohort study. *Stroke* 2016; **47:** 4–11.
26. Parkes LM, Rashid W, Chard DT, Tofts PS. Normal cerebral perfusion measurements using arterial spin labeling: reproducibility, stability, and age and gender effects. *Magn Reson Med* 2004; **51:** 736–743.
27. Chabriat H, Levy C, Taillia H, *et al*. Patterns of MRI lesions in CADASIL. *Neurology* 1998; **51:** 452–457.
28. Mitrajit G, Matilde B, Farida H, Martin D, Ute L, Nikolaus P. Pericytes are involved in the pathogenesis of cerebral autosomal dominant arteriopathy with subcortical infarcts and leukoencephalopathy. *Ann Neurol* 2015; **78:** 887–900.
29. Hall CN, Reynell C, Gesslein B, *et al*. Capillary pericytes regulate cerebral blood flow in health and disease. *Nature* 2014; **508:** 55–60.
30. Østergaard L, Engedal TS, Moreton F, *et al*. Cerebral small vessel disease: Capillary pathways to stroke and cognitive decline. *J Cereb Blood Flow Metab* 2016; **36:** 302–325.
31. Tuominen S, Miao Q, Kurki T, *et al*. Positron emission tomography examination of cerebral blood flow and glucose metabolism in young CADASIL patients. *Stroke* 2004; **35:** 1063–1067.
32. Mellies JK, Baumer T, Muller JA, *et al*. SPECT study of a German CADASIL family: a phenotype with migraine and progressive dementia only. *Neurology* 1998; **50:** 1715–1721.
33. Scheid R, Preul C, Lincke T, *et al*. Correlation of cognitive status, MRI- and SPECT-imaging in CADASIL patients. *Eur J Neurol* 2006; **13:** 363–370.
34. Yin X, Zhou Y, Yan S, Lou M. Effects of cerebral blood flow and white matter integrity on cognition in CADASIL patients. *Front Psychiatry* 2018; **9:** 741.
35. Ghezali L, Capone C, Baron-Menguy C, *et al*. Notch3-ECD immunotherapy improves cerebrovascular responses in CADASIL mice. *Ann Neurol* 2018; **84:** 246–259.
36. Chabriat H, Pappata S, Østergaard L, *et al*. Cerebral hemodynamics in CADASIL before and after acetazolamide challenge assessed with MRI bolus tracking. *Stroke* 2000; **31:** 1904–1912.
37. Ling Y, De Guio F, Jouvent E, *et al*. Clinical correlates of longitudinal MRI changes in CADASIL. *J Cereb Blood Flow Metab* 2019; **39:** 1299–1305.
38. Jefferson AL, Cambronero FE, Liu D, *et al*. Higher aortic stiffness is related to lower cerebral blood flow and preserved cerebrovascular reactivity in older adults. *Circulation* 2018; **138:** 1951–1962.
39. Mawet J, Vahedi K, Aout M, *et al*. Carotid atherosclerotic markers in CADASIL. *Cerebrovasc Dis* 2011; **31:** 246–252.
40. O'Leary DH, Bots ML. Imaging of atherosclerosis: carotid intima-media thickness. *Eur Heart J* 2010; **31:** 1682–1689.
41. Moreton FC, Dani KA, Goutcher C, O'Hare K, Muir KW. Respiratory challenge MRI: Practical aspects. *Neuroimage Clin* 2016; **11:** 667–677.

© 2020 The Authors. *European Journal of Neurology* published by John Wiley & Sons Ltd on behalf of European Academy of Neurology